Petroleum Science 19 (2022) 2905–2921

Contents lists available at ScienceDirect

Petroleum Science

journal homepage: www.keaipublishing.com/en/journals/petroleum-science

Original Paper

Discussion on the sweep efficiency of hybrid steam–chemical process in heavy oil reservoirs: An experimental study

Xiao-Hu Dong [a, *], Xiu-Chao Jiang [a], Wei Zheng [b], Hui-Qing Liu [a], Ren-Jie Liu [a], Wu-Chao Wang [a], De-Shang Zeng [a], Tai-Chao Wang [b]

[a] State Key Laboratory of Petroleum Resources and Prospecting, China University of Petroleum, Beijing, 102249, China
[b] State Key Laboratory of Offshore Oil Exploitation, Beijing, 100028, China

ARTICLE INFO

Article history:
Received 11 January 2022
Received in revised form
24 June 2022
Accepted 27 June 2022
Available online 30 June 2022

Edited by Yan-Hua Sun

Keywords:
Heavy oil reservoirs
Visualized model
Scaled 3D model
Sweep efficiency
Hybrid EOR process
Multicomponent and multiphase fluids

ABSTRACT

Non-condensable gas (NCG), foam and surfactant are the three commonly-used additives in hybrid steam–chemical processes for heavy oil reservoirs. Their application can effectively control the steam injection profile and increase the sweep efficiency. In this paper, the methods of microscale visualized experiment and macroscale 3D experiment are applied to systematically evaluate the areal and vertical sweep efficiencies of different hybrid steam–chemical processes. First, a series of static tests are performed to evaluate the effect of different additives on heavy oil properties. Then, by a series of tests on the microscale visualized model, the areal sweep efficiencies of a baseline steam flooding process and different follow-up hybrid EOR processes are obtained from the collected 2D images. Specifically, they include the hybrid steam–N_2 process, hybrid steam–N_2/foam process, hybrid steam–surfactant process and hybrid steam–N_2/foam/surfactant process (N_2/foam slug first and steam–surfactant co-injection then). From the results of static tests and visualized micromodels, the pore scale EOR mechanisms and the difference between them can be discussed. For the vertical sweep efficiencies, a macroscale 3D experiment of steam flooding process and a follow-up hybrid EOR process is conducted. Thereafter, combing the macroscale 3D experiment and laboratory-scaled numerical simulation, the vertical and overall sweep efficiencies of different hybrid steam–chemical processes are evaluated. Results indicate that compared with a steam flooding process, the areal sweep efficiency of a hybrid steam–N_2 process is lower. It is caused by the high mobility ratio in a steam–N_2–heavy oil system. By contrast, the enhancement of sweep efficiency by a hybrid steam–N_2/foam/surfactant process is the highest. It is because of the high resistance capacity of NCG foam system and the performance of surfactant. Specifically, a surfactant can interact with the oil film in chief zone and reduce the interfacial energy, and thus the oil droplets/films formed during steam injection stage are unlocked. For NCG foam, it can plug the chief steam flow zone and thus the subsequent injected steam is re-directed. Simultaneously, from the collected 2D images, it is also observed that the reservoir microscopic heterogeneity can have an important effect on their sweep efficiencies. From the 3D experiment and laboratory-scaled numerical simulation, it is found that a N_2/foam slug can increase the thermal front angle by about 15° and increase the vertical sweep efficiency by about 26%. Among the four processes, a multiple hybrid EOR process (steam–N_2/foam/surfactant process) is recommended than the other ones. This paper provides a novel method to systematically evaluate the sweep efficiency of hybrid steam–chemical process and some new insights on the mechanisms of sweep efficiency enhancement are also addressed. It can benefit the expansion of hybrid steam–chemical processes in the post steamed heavy oil reservoirs.

1. Introduction

Heavy oil refers to the liquid petroleum whose API gravity is less than 20° or viscosity is higher than 200 mPa s at reservoir conditions. Because of the high oil viscosity, steam injection processes

* Corresponding author.
E-mail address: dongxh@cup.edu.cn (X.-H. Dong).

https://doi.org/10.1016/j.petsci.2022.06.018

Nomenclature

C_i	Thermal capacity of water and rock (i = w, r), J/K
g	Gravitational acceleration, 7.32×10^{10} m/d^2
h	Reservoir thickness, m
i_s	Steam injection rate, m^3/d
K	Formation permeability, m^2
p_i	Pressure, Pa, (i = in, sc)
Q	Steam/gas injection volume, m^3
L	Model dimension, m
L_v	Latent heat of steam, kJ/kg
Q_i	Injection volume, m^3, (i = gin, gsc)
q	Production rate of drainage process, m^3/d
ΔS	Movable oil saturation (i.e., $S_{oi} - S_{or}$)
T_i	Temperature, K, (i = in, sc)
ΔT	Temperature difference between steam temperature and reservoir temperature, K
t	Production time, d
x	Steam quality
λ_r	Rock thermal conductivity, W/(m K)
μ	Oil viscosity, Pa s
ρ_i	Density of oil, water and rock, kg/m^3, (i = o, w, r)
$\Delta\rho$	Density difference between steam and condensate, kg/m^3
ϕ	Porosity

are usually the main exploitation methods for heavy oil reservoirs, e.g., cyclic steam stimulation (CSS), steam flooding, and steam assisted gravity drainage (SAGD) (Liu, 2013; Dong et al., 2019, 2021). But for the heavy oil reservoirs that have gone through a long-term stimulation of steam-based recovery processes, the underground fluid distributions and reservoir properties have changed significantly (Liu, 2013; Dong et al., 2017). And a series of problems have emerged and thus hindered the continuous normal development of heavy oil reservoirs, including steam override, steam breakthrough, fine migration, mineral dissolution, and water coning etc. (Mahmoudi et al., 2019; Sun et al., 2020; Dong et al., 2021). Simultaneously, the remaining oil saturation distribution in porous medium is also more complicated than its original status. It is dominated by not only the heavy oil reservoir properties but also the previous steam injection strategy. In a microscopic point of view, because of the effects of rock wettability, pore structure, microscopic heterogeneity, and *in-situ* emulsification, the remaining oil in porous medium can be usually classified into six categories, including membranous oil, columnar oil, multi-porous oil, cluster oil, emulsion oil droplets, and aggregation oil (Wang et al., 2021; Dong et al., 2021). By contrast, from a macroscopic aspect, the remaining saturation distribution is mainly dominated by the reservoir geological condition and operation scheme. Specifically, the recovery factor of a CSS process is about 20%–30%, and that of a steam flooding is about 40%–50% (Liu, 2013). Simultaneously, based on a sandpack experiment, the displacement efficiency of a steam injection process is about 70%–80%. Therefore, it indicates that the sweep efficiency of a CSS process in field is just about 28%–30%, and the sweep efficiency of a steam flooding process is about 61%–65%. Combing the microscopic and macroscopic remaining oil saturation distributions, it can be found increasing the sweep efficiency should be the most effective method for the continuous enhanced oil recovery (EOR) process of post steamed heavy oil reservoirs (Dong et al., 2021). Therefore, under such a requirement, hybrid EOR processes are proposed. Generally, the hybrid EOR processes in a heavy oil reservoir include a hybrid steam–NCG (non-condensable gas) process, a hybrid steam–solvent process, and a hybrid steam–chemical process (Ardali et al., 2012; Alvarez and Han, 2013; Ahmadi and Chen, 2020). Among them, compared with the additives of solvent and NCG, the application of chemical agents can significantly improve the steam injection profile and increase the sweep efficiency (Ahmadi and Chen, 2020). This indicates that for the heavy oil reservoirs with a serious phenomenon of steam breakthrough or steam fingering, a hybrid steam–chemical process should be the most recommended one.

For a hybrid steam–chemical process, the commonly used chemical additives include alkali, polymer, surfactant and foam. This process effectively combines the advantages of steam and chemical additives. Meanwhile, for different chemical additives, their EOR mechanisms are different (Pratama and Babadagli, 2022). First, the mechanisms of a hybrid steam–alkali process include emulsification, wettability alteration, interfacial tension (IFT) reduction and rigid film breaking (Dong et al., 2019). The commonly-used alkalis in hybrid EOR processes include Na_2CO_3 and NaOH. From an experimental investigation, it was found that a steam–alkaline process can effectively enhance the heavy oil recovery even under a low oil saturation condition (Okoye and Tiab, 1982; Tiab et al., 1982). But considering the formation damage behavior caused by alkaline, this process is rarely applied in field. Second, for polymer, it is usually applied in the non-thermal recovery process of heavy oil reservoirs. Especially for the offshore heavy oil reservoirs, considering the requirement of easily-operated facility, polymer is more attractive (Han et al., 2006; Dong et al., 2014). The SZ36-1 reservoir in Bohai offshore oilfield is one of the most successful polymer-based heavy oil EOR projects in the world (Dong et al. 2019). In recent years, Forberry (2013) and Taghavifar (2014) proposed a polymer-based hybrid process for heavy oil reservoirs, called Alkali-Co-Solvent-Polymer (ACP). In this process, alkali can benefit the reduction of interfacial tension, co-solvent can optimize the fluid phase behavior and polymer is used to increase the water viscosity. This process can well handle the challenges of injectivity, heating and oil displacement and production (Taghavifar, 2014; Dong et al., 2019). Third, for a steam–surfactant process (HSSP), it can significantly improve the properties of fluid-fluid interface and fluid-rock interface. The commonly used surfactants in a HSSP include anionic, non-ionic cationic and amphoteric (Ahmadi and Chen, 2020). The EOR mechanisms include oil viscosity reduction, wettability alteration, IFT reduction and *in-situ* emulsification (Ko et al., 2014; Wu et al., 2018; Dong et al., 2019; Bashir et al., 2021). Especially, for the post steamed heavy oil reservoirs, under the effect of emulsion droplets, a HSSP process can effectively plug the steam breakthrough path and thus increase the sweep efficiency (Wang et al., 2021). Specifically, by using a microscopic etched glass model, Liu et al. (2022) experimentally discussed the emulsification mechanisms of surfactant flooding in heavy oil reservoirs. It was found that the three effects can dominate the entire flooding process, including cutting emulsification, peeling-off emulsification, and temporary blocking. Their experimental observation further clarified that the improvement of surfactant system on the sweep efficiency of heavy oil reservoirs. Last, for an NCG-foam system, it is usually applied to increase the viscosity of gas phase, reduce the gas mobility and finally increase the sweep efficiency. NCG-foam is a dispersion system in which the surfactant solution is a continuous phase, and NCG (N_2, CO_2, CH_4) is a dispersed phase (Pang et al., 2015; Jia et al., 2018). Wang et al. (2015) experimentally

discussed the application of N_2-foam system in the heavy oil reservoirs with bottom water. It is found that the injection of N_2-foam can also effectively plug the water coning path and thus improve the oil recovery. On the other hand, for the post steamed heavy oil reservoirs, the injection of foaming agent can also enhance the strength of dispersed gas phase, and thus the dispersed gas phase can plug the steam breakthrough path (Wang et al., 2018; Dong et al., 2021). In recent years, some researchers have proposed that the nanoparticles can be applied as a foam stabilizer in the thermal recovery processes (Khajehpour et al., 2016; Maaref and Kantzas, 2022). After the co-injection of water containing nanoparticles, a significant improvement on the mobility factor reduction and steam control can be observed. In summary, compared with a hybrid steam–NCG process, an NCG–foam system usually has a higher sweep efficiency (Delamaide et al., 2016; Liu et al., 2016).

Based on the discussion above, it can be found that the hybrid steam–chemical processes can not only effectively utilize the residual heat energy after steam injection but also significantly increase the sweep efficiency from different aspects. Currently, they have been widely applied to enhance the heavy oil recovery in the world, especially for the hybrid steam–surfactant and steam–NCG/foam processes (Dong et al., 2019). In Canada, some polit tests by using the processes of HSSP, surfactant assisted-SAGD (SA-SAGD) and hybrid alkali steam process (HASP) have been reported. In China, an oil viscosity reducer (VR) or an oil displacement agent has been selected as the surfactants to apply in a hybrid steam–surfactant process, and they have been successfully piloted in Shengli, Liaohe, Henan and Xinjiang oilfields (Huo et al., 1999; Zhang and Zhao, 2007; Liu, 2013). On the other hand, for the application of NCG–foam injection process, it can back to the 1980s (Keijzer et al., 1986; Mendez et al., 1992). From that time on, this process has been gradually applied to improve the recovery performance of steam-based processes, including CSS and steam flooding processes (Shi et al., 2005; Bi et al. 2014). In recent years, the NCG foam system has been also proposed to improve the SAGD performance (Dong et al., 2014; Adetunji et al., 2019; Delamaide et al., 2020). The injection of an NCG–foam slug can effectively enhance the oil recovery factor even at a residual oil saturation condition (Dong et al., 2019, 2021). After a systematic literature review, although the different hybrid steam–chemical processes have been widely applied in the heavy oil production process, an evaluation method on the effect of hybrid EOR processes on the sweep efficiency is still lacking. Therefore, in order to further expand the field application of hybrid thermal–chemical processes in heavy oil reservoirs, there is an urgent requirement on a systemic discussion of the sweep efficiency enhancement behavior of hybrid steam–chemical processes.

In this paper, the reservoir sweep efficiencies of a heavy oil reservoir are classified into areal and vertical sweep efficiencies. By using the methods of microscale visualized experiment and macroscale 3D experiment, they are experimentally evaluated. In Section 2, the detailed experimental setup and procedure are provided, including the static evaluation tests, visualized experiment and scaled 3D experiment. In Section 3, the detailed experimental observation and the laboratory-scaled numerical simulation results are provided. Simultaneously, discussion on the EOR mechanisms of different hybrid steam–chemical processes is also provided in this section. In Section 4, the main concluding remarks are drawn.

2. Experimental method

2.1. Experimental materials

In this study, we respectively performed the following experiments, the static evaluation tests of chemicals, microscale visualized experiments and scaled 3D experiments. The chemical agents used in this study include two foaming agents (main chemical composition: sodium dodecyl sulfate, SDS) and an oil soluble surfactant (main chemical composition: ethylene-vinyl acetate copolymer). All of them have been applied in the heavy oil recovery processes in Xinjiang Oilfield, CNPC. On the other hand, the surfactant applied is also a typical oil displacement chemical agent, and it has an obvious effect on reducing the oil viscosity. Therefore, it is also called as a viscosity reducer (VR). The oil samples used in this study is a wellhead dead oil from a typical thermal well in Xinjiang Oilfield. The curve between oil viscosity and temperature is shown in Fig. 1. The initial formation temperature is 42 °C.

The water sample used to establish the initial fluid saturation distribution is a synthetic simulated formation water according to the actual ionic composition of formation water, as shown in Table 1. The total salinity is 6524 ppm.

2.2. Static evaluation tests of chemicals

For the static evaluation tests of chemicals, they can play a more important role for the successful operation of a hybrid steam–chemical process in heavy oil reservoirs. First, for a foaming agent, the properties of pH value, maximum foaming volume and half-life period are the three commonly-used static indicators to evaluate its preformation. In this study, the maximum foaming volume and half-life period is firstly evaluated by using the Waring Blender method (Sun et al., 2014; Lu et al., 2013). It is the commonly-used method to evaluate the static performance of foaming agent. Simultaneously, the pH value of the foaming agent solution is also tested. For the blocking behavior of NCG/foam system, a sandpack model is applied. The detailed experimental procedure can be found in some of our previous publications (Wang et al., 2012; Lu et al., 2013). Thus, based on the static performance and the blocking behavior of foaming agent, an optimal foaming agent can be selected.

On the other hand, for surfactant (VR), the IFT between heavy oil and surfactant solution is firstly tested by a SVT20N rheometer. Simultaneously, considering the degradation behavior of chemical agent at high temperature condition, its IFT after high temperature treatment for different times are also tested. During tests, the mass concentration is always controlled at 0.5 wt%, the tolerable temperature is 250 °C, and the test temperature is 50 °C. After a high temperature treatment, the viscosities of heavy oil sample and the mixture of heavy oil and surfactant solution are tested. For this

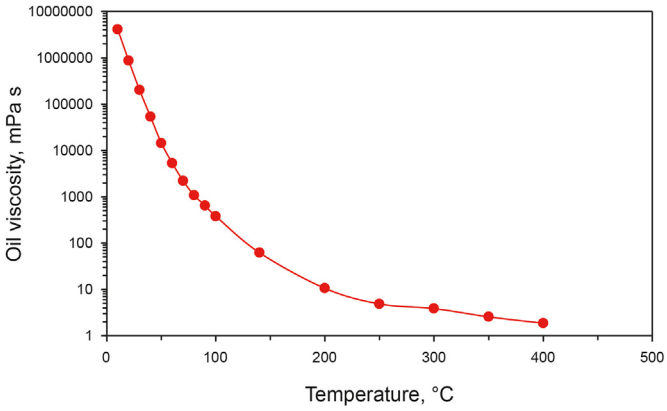

Fig. 1. Oil viscosity vs. temperature.

Table 1
The ionic composition of formation water.

Ionic composition	Ca^{2+}	HCO_3^-	SO_4^{2-}	Cl^-	Mg^{2+}	Na^+
Concentration, ppm	764	473	1080	5330	648	4736

mixture, the ratio of heavy oil sample and surfactant solution is 7:3. The mixture viscosity can be used to effectively evaluate the behavior of oil viscosity reduction of this surfactant during a hybrid EOR process.

2.3. Microscale visualized experiments

Based on the results of static evaluation tests, a series of microscale visualized experiments are performed, including the steam flooding process, hybrid steam–N_2 process, hybrid steam–N_2/foam process and hybrid steam–surfactant process. Different from the method of etch chips, the microscale visualized models used in this study is a glass bead micro-model (Dong et al., 2021; Wang et al., 2021). For etch chips, the pores and throats are usually simulated by different categories of grooves on glass, and they have a low-pressure capability. Simultaneously, the temperature resistance of etch chips is low (Dong et al., 2021). Thus, they are rarely applied to simulate the thermal recovery process of heavy oil reservoirs. In this paper, a new micromodel is developed by two high-pressure quartz glass sheets with a length of 25 cm. Between the two glass sheets, one or two layers of glass beads were filled to simulate a porous medium environment. The glass bead used in this study has a diameter of 0.6 mm (40 mesh). One of the glass sheets is equipped with a penetrating hole to simulate the well. The size of the visual area is 20 cm × 20 cm. On the other hand, in order to simulate the conditions of high temperature and high pressure, a glass cement is applied to seal the glass sheet and silicone plate.

A schematic for the microscale visualized experimental procedure is shown in Fig. 2. As shown, it is composed of a visualized model, an image acquisition system, a temperature control box, a data acquisition system, and a fluid injection and acquisition system. For the porosity of this micro-model, it can be obtained by a water injection process. In this study, the porosity of this model is about 32.26%. For its permeability, it can be determined by a sandpack model using the same glass bead. After test, it is about 2100×10^{-3} μm^2. During experiments, a digital camera and a Sweden optical microscope (magnification: ~800 times) are placed in front of the visualized model to obtain the real-time images. Meanwhile, a plane light source is also placed on the back of the visualized model to benefit the image collection process.

Table 2 gives the detailed operation parameters of the visualized experiments. During experiments, the steam temperature is 200 °C, and the steam quality is 0.8. For the four hybrid recovery processes, the foaming agent solution has a weight concentration of 0.5 wt%, the surfactant solution has a same weight concentration of 0.5 wt%. The N_2 injection rate is controlled by a constant gas flow meter at the standard condition. For hybrid steam–N_2 process and hybrid steam–surfactant process, the steam and additive will be co-injected simultaneously. For hybrid steam–N_2/foam process, a N_2/foam slug (0.1 PV) is firstly injected, and then the subsequent steam injection process is performed. For hybrid steam–N_2/foam/surfactant process, a N_2/foam slug (0.1 PV) is firstly injected, and then the steam and surfactant solution are co-injected into the micromodel. The detailed experimental procedures are as follows:

(1) Prepare the microscale visualized model and connect the experimental device;
(2) Inject nitrogen into the visualized model, maintain at the pressure of 0.5 MPa for about 30 min to test the gas leakage of this model;
(3) Set the oven temperature at reservoir temperature (50 °C);
(4) Inject prepared formation water into the visualized model to test the model porosity;
(5) Inject heavy oil sample into the visualized model to develop the initial oil saturation distribution;
(6) Keep this model at reservoir temperature condition for 24 h;
(7) Inject steam into the micromodel until a steam breakthrough path is observed;
(8) Proceed the hybrid EOR process according to the experimental design (see Table 2) until the designed volume of chemical slug is achieved, and then re-activate the 2nd steam injection process.

2.4. Macroscale 3D experiment

Macroscale 3D experiment is a commonly-used method to simulate some complicated physical phenomena in laboratory by a scaled model. In this paper, a 3D model is applied to simulate the recovery process of different hybrid steam–chemical processes in heavy oil reservoirs. The 3D model used in this study has an inner space of 40 cm × 40 cm × 40 cm. The affordable pressure condition is 10 MPa. In order to reduce the heat loss between 3D model and environment, the inner surface of this 3D model is covered by a heat insulation material. A schematic for the experimental procedure is shown in Fig. 3. It can be classified into five subsystems, i.e., injection system, 3D physical model, production system, data acquisition system, and auxiliary system.

For the detailed experimental parameters, a similarity criterion can play a more important role for macroscale 3D experimental process. Table 3 provides the similarity criterion used in this paper. Thus, from this similarity criterion, the experimental parameters can be obtained based on the actual reservoir properties of a typical heavy oil reservoir in Xinjiang Oilfield, CNPC, as shown in Table 4. In the 3D experiment, 1/4 of a five-spot well pattern in this actual heavy oil reservoir is simulated.

The detailed experimental procedures are as follows.

(1) 3D model construction. The earthenware clay is applied in the inner surface of this 3D model to prevent the steam breakthrough along the model surface. Simultaneously, this model setting can also increase the thermal efficient of hot fluids.
(2) Quartz sand filling process. Firstly, by using a sandpack model with a length of 35 cm and a diameter of 3.8 cm, the permeability of quartz sand with different meshes is tested. The results are shown in Fig. 4 (Dong et al., 2022). Then, combining the requirement of 3D model permeability in Table 3, the quartz sand with the mesh of 20 can be used. Thus, from the geometrical properties of this 3D model, the total quartz sand volume during the experiment can be obtained ($40 \times 40 \times 10$ cm^3). Simultaneously, it is assumed that the porosity of this porous medium is about 30%, thus the total fluid volume can be obtained. Thereafter, the quartz sand can be mixed with water and oil to prepare the oil sand samples. During the mixing process, considering the wettability of quartz sand, it is assumed that the irreducible water saturation is about 20%. Therefore, the ratio of oil volume and water volume is 4:1. Then the prepared oil sand sample is filled within the 3D model. During the sand filling process, 36 temperature transducers (3×12) are installed within the 3D

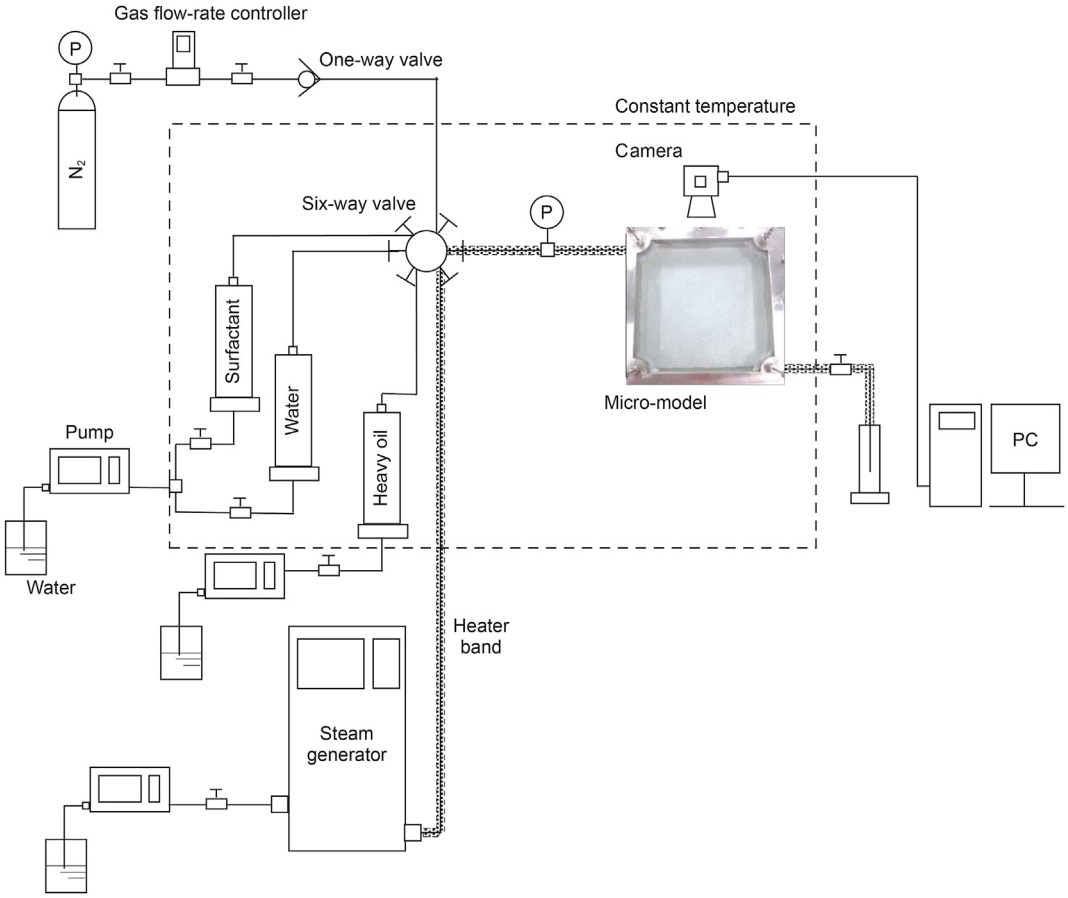

Fig. 2. Schematic diagram of visualized experiment.

Table 2
Experimental parameters of microscale visualized experiments.

No.	Method	1st steam injection rate, mL/min	Stages to improve the sweep efficiency			2nd steam injection rate, mL/min
			N_2 injection rate, mL/min[a]	Foaming agent solution injection rate, mL/min	Surfactant solution injection rate, mL/min	
1#	Baseline steam injection process	0.5	–	–	–	–
2#	Hybrid steam–N_2 process	0.5	5	–	–	0.5
3#	Hybrid steam–N_2/foam process	0.5	5	0.5	–	0.5
4#	Hybrid steam–surfactant process	0.5	–	–	0.5	0.5
5#	N_2/foam slug first and steam–surfactant co-injection then	0.5	5	0.5	0.5	0.5

[a] Standard condition.

model. It can be used to test the temperature distribution in real-time.

(3) Fluid saturation offset process. After the oil sand filling process, the 3D model is placed into a constant temperature oven, and its temperature is set at the reservoir temperature (30 °C). Then, water and oil are simultaneously injected into the 3D model under the ratio of 4:1. On the other hand, in order to guarantee that all the pore space can be fully saturated, the fluid injection ports should be changed during the process. Once the fluid composition is no longer changed, the fluid saturation process is terminated. Then, this model is kept in the reservoir temperature condition for 48 h.

(4) CSS process. Based on the experimental parameters in Tables 4 and 5 CSS cycles are firstly simulated. Both the two wells are simultaneously performing the process of steam injection (15 min), soaking (3 min) and production (20 min).

(5) Steam flooding process. The steam is continuously injected at a rate of 15 mL/min. Once an obvious steam breakthrough is observed, it is terminated.

(6) N_2/foam slug injection process. The N_2 and foaming agent solution are co-injected from injection well. The injection rate of N_2 is 10 mL/min at standard conditions. The injection rate of foaming agent solution is 2 mL/min. Once the designed foam injection volume (0.1 PV) is achieved, the injection process is terminated.

(8) Second steam flooding process. The steam injection process is re-activated at the steam injection rate of 15 mL/min. Once

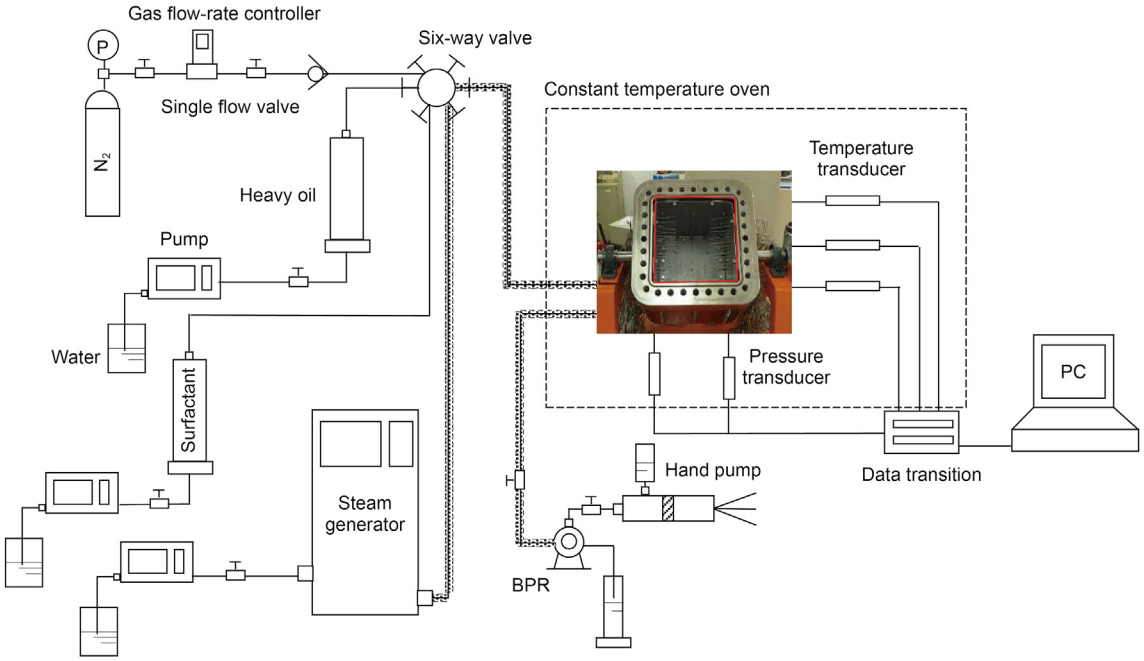

Fig. 3. Schematic diagram of 3D experiment.

Table 3
Similarity criterion of steam injection process for heavy oil reservoirs.

Stage	Similarity criterion	Physical meaning	Simulation parameter
Fundamental parameters	$\pi_1 = \frac{K\rho_o gt}{\phi\Delta S\mu L}$	Ratio of gravity to viscous force	Permeability
	$\pi_2 = \frac{xL_v}{C_w\Delta T}$	Ratio of energy loss to injected energy	Steam quality
	$\pi_3 = \frac{\lambda_r t}{\rho_r C_r L^2}$	Ratio of conductivity to heat capacity	Time
CSS	$\pi_4 = \frac{Kt}{\mu c\phi L^2}$	Dimensionless elastic energy	Compressibility
	$\pi_5 = \frac{\Delta\rho gKt}{\mu L}$	Ratio of gravity to viscous force	CSS cycle
Steam flooding	$\pi_6 = \frac{\Delta p}{\rho_o gL}$	Ratio of pressure to gravity	Pressure difference
	$\pi_7 = \frac{i_s t}{\phi\Delta S\rho_w L^3}$	Dimensionless injected mass	Steam injection rate
Hybrid steam–N_2/foam process	$\pi_8 = \frac{p_{in}\, T_{sc} Q_{gin}}{p_{sc} T_{in}\, Q_{gsc}}$	Steam/gas ratio	Gas injection rate

the water cut reaches above 98%, the entire experiment process is terminated.

3. Results and discussion

3.1. Results of the static evaluation tests

3.1.1. Properties of foaming agent

(1) Foaming volume and hall-life period of foaming agent solution

In this study, two different foaming agents are tested. Fig. 5 shows the pH values of the two foaming agent solutions with different concentrations. As shown, with the mass concentration increases, the pH value increases gradually. Once the mass concentration reaches above 0.5 wt%, the pH value is relatively stable. Comparatively, the foaming agent 1# is alkalescent, and the other one is weakly acidic.

Fig. 6 gives the results of foaming volume and hall-life period. As shown, with the mass concentration increases, both the foaming agent and hall-life period can show a tendency of increase first and reduce then. As the mass concentration reaches 0.5 wt%, a maximum value can be observed. Simultaneously, foaming agent 1# performs better than foaming agent 2#.

(2) Blocking behavior of N_2/foam system

Blocking behavior is one of the most important indexes to evaluate the performance of an NCG–foam system in porous medium. Resistance factor is a commonly-used parameter to evaluate the blocking behavior of foam system. The experimental results for the resistance factor of foaming agent solution at different conditions are shown in Fig. 7. Similarly, with the mass concentration increases, the resistance factor is gradually increased. As the concentration is greater than about 0.5 wt% (critical micelle concentration), the increasing tendency is reduced. But for the results at different temperature conditions, the two foaming agents show

Table 4
Experimental parameters.

Stage	Parameter	Prototype	3D model
Basic data	Wellbore radius	0.1 m	0.3 cm
	Pay thickness	15 m	10 cm
	Porosity	33%	33%
	Permeability	5 μm^2	40 μm^2
	Original oil saturation	80%	80%
	Initial water saturation	20%	20%
	Oil viscosity @ 50 °C	23357 mPa s	23357 mPa s
	Reservoir temperature	30 °C	30 °C
	Steam temperature	250 °C	250 °C
	Steam quality	0.7	0.7
	Initial pressure	3.4 MPa	3.4 MPa
CSS phase	Steam injection rate	200 t/d	40 mL/min
	Total steam injection volume	2000 t	400 mL
	CSS cycle	5	5
	Shut-in time	3 d	2 min
	Production time	120 d	20 min
Steam flooding phase	1st steam injection rate	200 t/d	15 mL/min
	Steam injection time	1 year	20 min
Hybrid steam–chemical process	N_2 injection rate	500 t/d	10 mL/min
	Concentration of foaming agent solution	0.5 wt%	0.5 wt%
	Foaming agent injection rate	2.67 t/d	2 mL/min
	2nd steam injection rate	200 t/d	15 mL/min

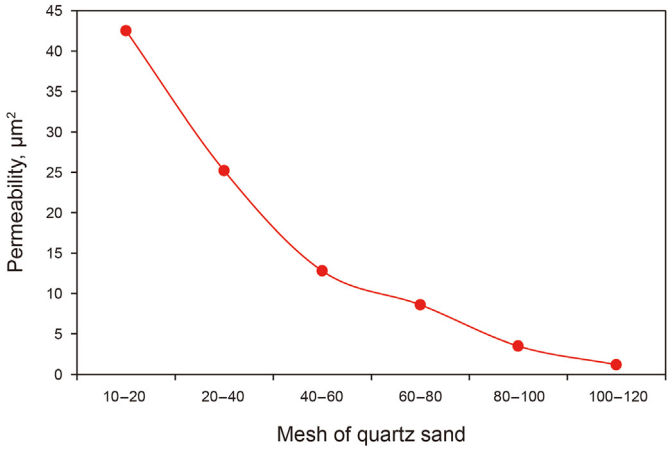

Fig. 4. Permeabilities of the quartz sand with different mesh.

different changing characteristics. For foaming agent 2#, as the temperature increases, the resistance factor is steadily increased. Even as the temperature is higher than 200 °C, the N_2/foam system can still present a reliable blocking behavior. But for foaming agent 1#, it shows a different tendency of increase first and reduce then. As the temperature is higher than 100 °C, the resistance factor is reduced. This indicates that this foaming agent cannot tolerate a high temperature condition. Therefore, combining all the test results, foaming agent 2# is recommended, and it can be applied to perform the subsequent experiments.

3.1.2. Properties of surfactant (VR)

Firstly, the IFTs between heavy oil sample and VR solution at different conditions are tested, the results are shown Fig. 8. As shown, with the test time increases, the IFT is gradually stabilized. On account of the effect of degradation behavior at high temperature condition, the IFT of VR solution after high temperature treatment increases. In this study, the temperature is 250 °C, and we respectively test the IFTs of VR solution after high temperature treatment for different times. From Fig. 8, it can be observed that as the duration time of high temperature is above 5 d, the IFT is relatively stable. Compared with the initial state, after 7 d of duration at high temperature condition, its IFT is just increased from 0.16 to 0.22 mN/m. This indicates that this surfactant shows a good thermal stability.

Fig. 9 shows the viscosities of heavy oil and the mixture of heavy oil and VR solution. As shown, on the basis of high temperature condition, the addition of VR solution can further reduce the heavy oil viscosity. But comparatively, as the temperature is low (<100 °C), the behavior of oil viscosity reduction caused by surfactant is more significant. When the temperature rises to a higher value, the oil viscosity has already reached to a low value. This indicates that the effect of surfactant on the oil viscosity is limited. On the other hand, in order to effectively evaluate the behavior of oil viscosity reduction of VR solution, a new parameter is proposed, viscosity reduction ratio, as shown in Eq. (1). Therefore, from Fig. 9, it can be observed that the effect of temperature on the viscosity reduction ratio is significant.

Table 5
Sweep efficiencies of different hybrid processes.

No.	Process	Sweep efficiency, %		Final sweep efficiency, %	Incremental sweep efficiency, %
		1st steam flooding process	Hybrid steam–chemical process		
1#	Baseline steam injection process	20.16	–	20.16	–
2#	Hybrid steam–N_2 process	–	18.69	18.69	−1.47
3#	Hybrid steam–N_2/foam process	20.16	23.25	28.57	8.41
4#	Hybrid steam–surfactant process	19.92	30.12	30.12	10.20
5#	N_2/foam slug first and steam–surfactant co-injection then	16.43	19.51	33.19	16.76

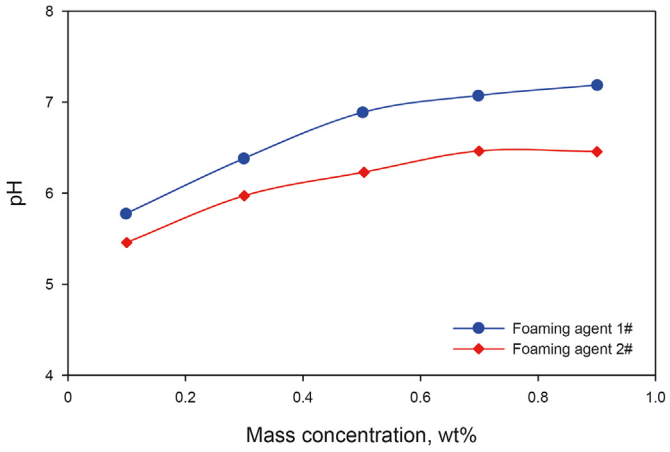

Fig. 5. Results of the pH values of foaming agent solution.

$$f = \frac{\mu_0 - \mu}{\mu_0} \times 100\% \quad (1)$$

where μ_0 and μ respectively refer to the viscosities of the heavy oil and the mixture, respectively.

3.2. Results of the microscale visualized experiments

Based on the above static evolution tests, applying the methods above, five different sets of microscale visualized experiments are performed, as shown in Table 2. For the processes of hybrid steam–N_2 injection and hybrid steam–surfactant solution injection, the steam and additives will be co-injected into the model. But for the other two processes (4# and 5#), a chemical slug is injected firstly and the subsequent steam injection is activated then.

3.2.1. Pure steam injection process

For the different microscale visualized experiments, by collecting the camera images at different operation times, the swept area of different hybrid thermal–chemical processes can be obtained. Thus, the areal sweep efficiency can be easily calculated through the grayscale and binarization images. Fig. 10 shows the collected images of steam injection process. As the steam is injected into the micromodel, the swept area is gradually expanded. For each image, the bright color range refers to the steam flow path (swept area), and the dead color area refers to the unswept range. It can be found

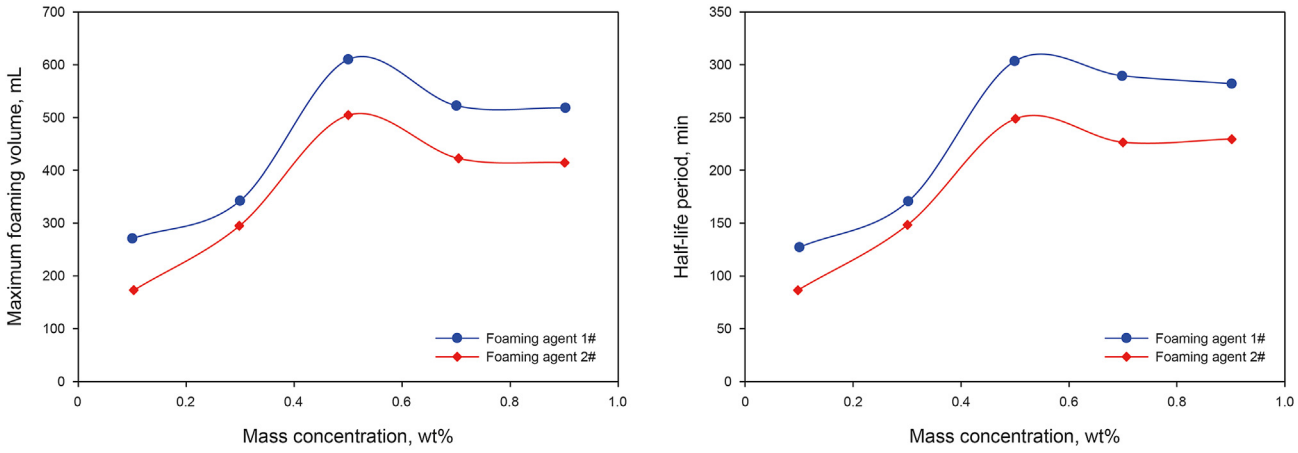

(a) Maximum foaming volume

(b) Half-life period

Fig. 6. Results of the foaming volume and hall-life period of foaming agent solution.

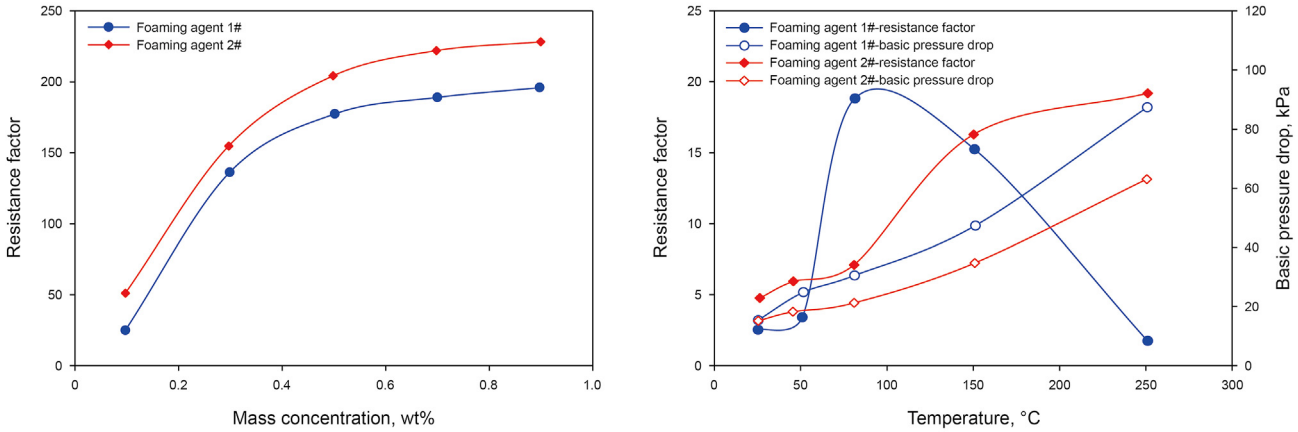

(a) Effect of mass concentration

(b) Effect of temperature

Fig. 7. Results of the resistance factor of N_2/foam system.

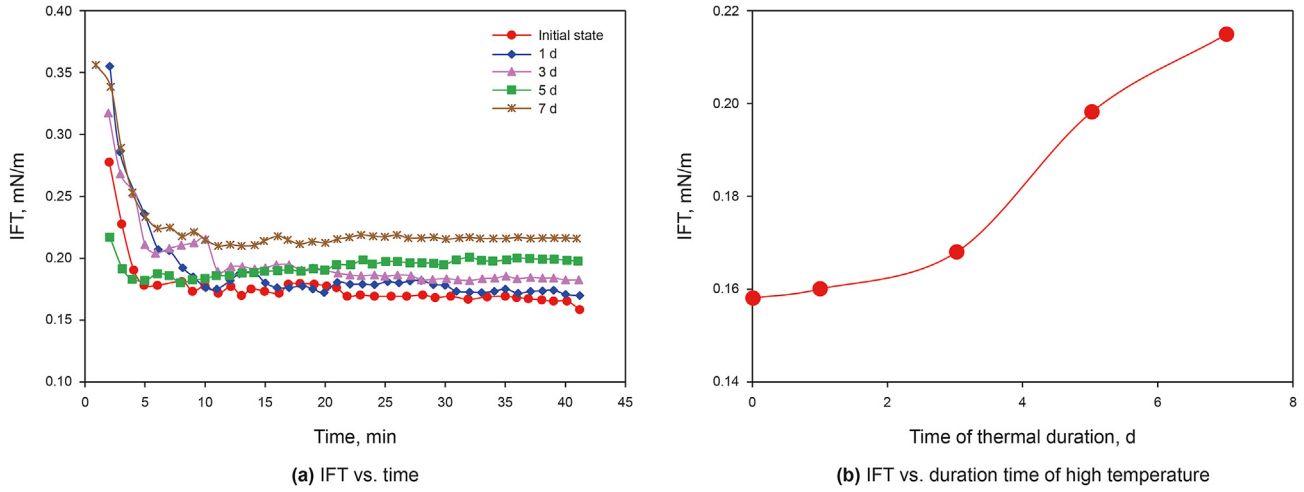

Fig. 8. IFTs between heavy oil sample and VR solution.

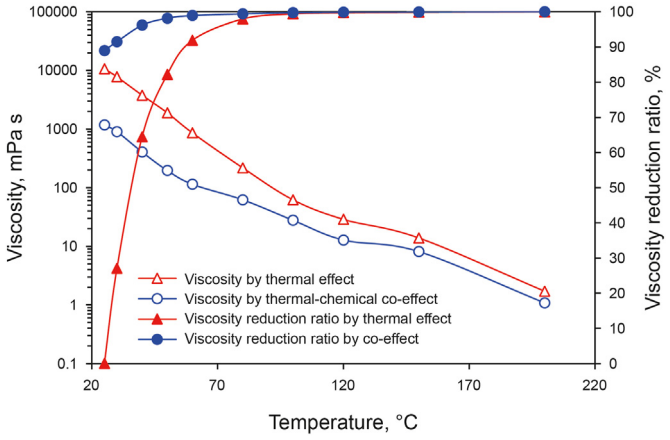

Fig. 9. Viscosities of heavy oil and mixture of heavy oil and VR solution.

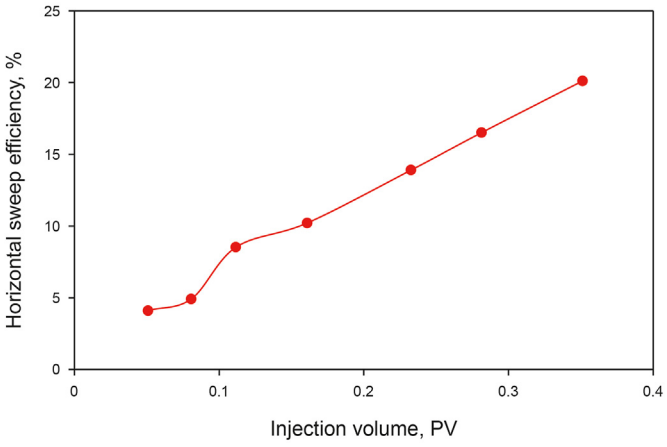

Fig. 11. Horizontal sweep efficiency of pure steam injection process.

that once the total injection volume achieves about 0.38 PV, an obvious steam breakthrough path can be observed. And the steam injection process is terminated. Then, based on the grayscale and binarization images, the sweep efficiencies of steam injection process at different times can be obtained, as shown in Fig. 11. The areal sweep efficiency of pure steam injection process is about 20.16%. Although the steam injection process is stopped, there is still large amount of unswept area, and the potential of hybrid EOR processes is high.

3.2.2. Hybrid EOR processes

Fig. 12 shows the results of the four different hybrid steam–chemical processes. As shown, on the basis of steam injection process, the implementation of hybrid processes can effectively increase the swept area. Table 5 provides the calculated sweep efficiencies.

First, for hybrid steam–N_2 process (2#), because of the low solubility of N_2 in heavy oil, once N_2 is injected into the reservoir, it can present the gas bubble flow behavior. And simultaneously, N_2 mainly moves along the previous steam breakthrough path. Thus,

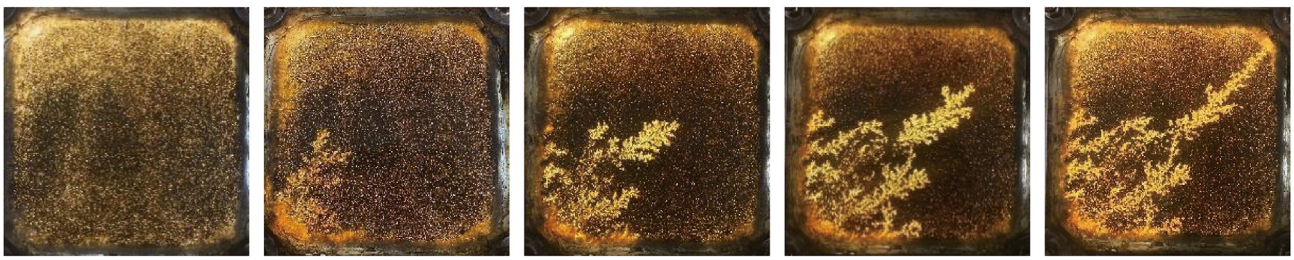

Fig. 10. Steam injection process at different times.

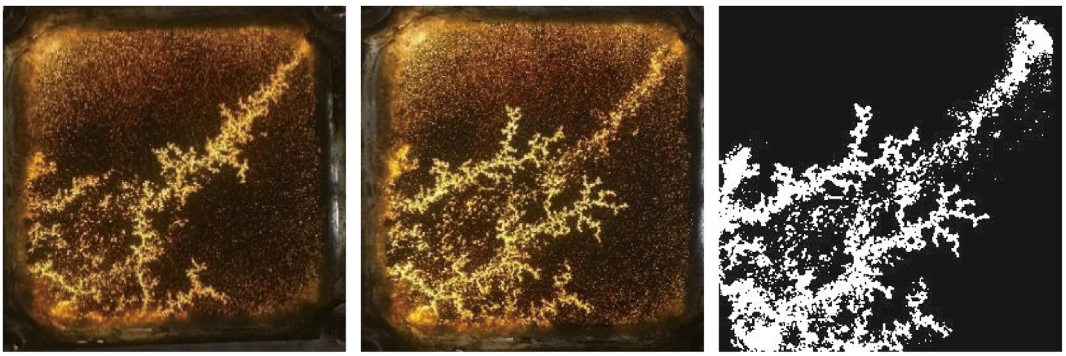

(a) Hybrid steam–N_2 injection process

(b) N_2/foam plug injection and subsequent steam flooding process

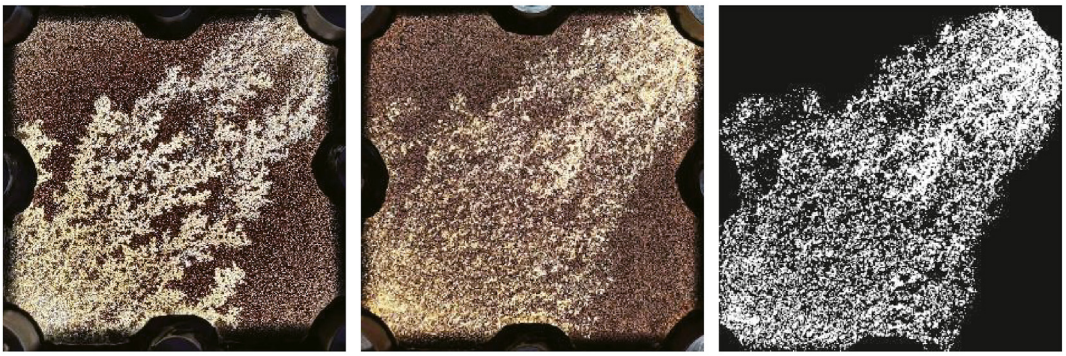

(c) Hybrid steam–surfactant injection process

(d) N_2/foam/surfactant injection and subsequent steam flooding process

Fig. 12. Results of four different hybrid steam–chemical processes.

the steam breakthrough characteristics can be enhanced to some content. Based on the binarization image after hybrid steam–N_2 process in Fig. 12(a), it can be calculated that the final sweep efficiency of this case is about 18.69%. On the basis of pure steam injection process, the operation of hybrid steam–N_2 process even reduces the sweep efficiency by 1.47% (see Table 5). It is mainly caused by the higher mobility ratio between N_2 and heavy oil in a hybrid steam–N_2 process.

Second, for N_2/foam injection process (3#), the plugging strength of foam system is higher than that of N_2. A stable foam system can effectively plug the steam breakthrough path and increase the swept area. Similar to the hybrid steam–surfactant process, under the effect of chemical agent (foaming agent), the fluid contact relationship will change from an unstable gas (N_2)/oil interface to a stable gas (N_2)/chemical/oil interface. It can significantly enhance the plugging strength of gas bubble. Thus, after a subsequent steam flooding process, the recovery performance can be improved. From the binarization image in Fig. 12(b), for this case, the final sweep efficiency after subsequent steam flooding process is about 28.57%. From Table 5, it is increased by 8.41% than the baseline steam injection process (in this case, the sweep efficiency of steam injection process is 20.16%).

Third, for hybrid steam–surfactant process (4#), based on the test results of static evaluation, the surfactant used in this study (VR) has an obvious effect on oil viscosity reduction. Simultaneously, it can also present a good performance at the steam temperature condition. For hybrid steam–surfactant process, *in-situ* emulsification is one of the most important EOR mechanisms. Therefore, with the injection of surfactant solution, the contact relationship between oil and water will change from a water/oil interface to water/chemical/oil interface. It can benefit the reduction of interfacial energy and the enhancement of oil recovery. From the binarization image in Fig. 12(c). it can be observed that after the hybrid EOR process, the final sweep efficiency is about 30.12%. From Table 5, it is increased by 10.20% than the baseline steam injection process (in this case, the sweep efficiency of pure steam injection process is 19.92%).

Last, for N_2/foam/surfactant injection process (5#), this process can simultaneously play the advantages of N_2/foam system and surfactant solution. Under the effect of foam blockage and surfactant *in-situ* emulsification, the swept area can be largely improved. As shown in Fig. 12(d), the final sweep efficiency after subsequent steam flooding process is about 33.19%. From Table 5, it is increased by 16.76% than the baseline steam injection process (in this case, the sweep efficiency of pure steam injection process is 16.43%). In summary, among the four different hybrid EOR processes, the areal sweep efficiency of a hybrid N_2/foam/surfactant process is the highest. This process can fully play the advantages of foam and surfactant systems.

3.2.3. Effect of the microscopic reservoir heterogeneity

From Figs. 10 and 12, it can be found that the microscopic reservoir heterogeneity can significantly affect the recovery performance. As shown, within the fluid swept area, although some pore space still presents the dark color. It indicates that the porous range is not swept, and when the displacing fluid front reaches to this area, a fluid bypass behavior can be observed. On the other hand, if this effect caused by a microscopic reservoir heterogeneity can be neglected, it can be found the calculated sweep efficiency is tremendously improved. As shown in Fig. 13, based on the binarization images at the end of each experiment, we can calculate the sweep efficiencies with and without the consideration of microscopic reservoir heterogeneity. For the sweep efficiency without the consideration of microscopic reservoir heterogeneity, it actually can be calculated based on an area ratio, as shown below.

$$E_s = \frac{A_S}{A} \tag{2}$$

where E_s is the sweep efficiency; A_S is the swept area (marked by the red line) (see Fig. 13); A is the entire oil-bearing area.

The calculated results are shown in Fig. 14. It can be found that the microscopic reservoir heterogeneity has a significant effect on the areal sweep efficiency. Compared with the calculated results with the consideration of heterogeneity, the sweep efficiency by neglecting the effect of heterogeneity is almost doubled.

3.3. Results of the macroscale 3D experiment

3.3.1. Experimental results & discussion

In Section 3.2, the areal sweep efficiencies of different hybrid thermal–chemical processes are discussed from the microscale visualized experiments. In this section, the vertical sweep efficiency will be addressed based on the 3D experiment and its correspondingly laboratory-scaled numerical simulation.

Figs. 15 and 16 respectively show the results of liquid production and temperature distribution. As shown, both wells simultaneously perform 5 CSS cycles. During the entire 3D experiment, the total oil production volume is 3360 mL, and the total heavy oil volume saturated is 5800 mL. From Fig. 15, it can be found that after the CSS recovery process (250 min), the oil recovery factor has reached 17.5%. Combing the temperature observation results in Fig. 16, the reservoir region around the well has been effectively heated. Thus, it can be transferred to a steam flooding process. During the steam flooding process, steam is continuously injected into the reservoir, and thus the reservoir region between the two wells can be effectively unlocked. From Fig. 15, as the operation time reaches about 330 min, a steam breakthrough phenomenon between injector and producer is observed. At this time, a sudden reduction on the oil production rate can be found and the recovery factor is about 17.5%. Then, as the operation time reaches about 440 min, the steam flooding process is terminated (oil recovery factor: 24.3%) and a N_2/foam slug (0.1 PV) is injected. Then applying the same steam injection rate, the 2nd steam flooding process is performed. From Figs. 15 and 16, after a N_2/foam slug is injected, both the oil production rate and cumulative oil/steam ratio are obviously increased. It is because that the N_2/foam slug has effectively plugged the previous steam breakthrough path, and the steam injection front is improved. As shown in Fig. 16, under the effect of N_2/foam slug, the steam injection front angle is increased from 35° to 50°. Finally, the oil recovery factor reaches about 57.9%.

3.3.2. Laboratory-scaled numerical simulation

(1) Laboratory-scaled numerical simulation model development

3D experiment is an expensive and time-consuming simulation process. In contrast, after a sufficient scaling design and simulation, a laboratory-scaled numerical simulation can provide an effective method to replace the 3D experiment. Therefore, in this section, based on the above 3D experimental results, using the same data setting in Table 4, a laboratory-scaled numerical simulation model is developed. As shown in Fig. 17, this model has a 25 × 25 × 29 grid system (52 cm × 52 cm × 40 m). In order to accurately simulate the properties of 3D model, 4 groups of thermal parameters are used in the laboratory-scaled numerical simulation model, i.e., iron model surface, thermal insulating layer, clay (cap rock) and oil reservoir. Then, based on this model, a series of numerical simulation runs are performed to history match the experimental measurements. During this process, we mainly modify the parameters of relative permeability curve and wellbore parameters (well index and skin factor). Fig. 18 compares the results of the 3D physical model and the final numerical simulation model. As shown, the numerical simulation results are in good agreement with the experimental observation. The ultimate oil recovery factors of experimental and numerical results are 58.5% and 61.3%, respectively. The relative error is just about 4.78%. Meanwhile, the results of cumulative oil/steam ratio and oil production rate of this numerical simulation model also match the experimental data very well.

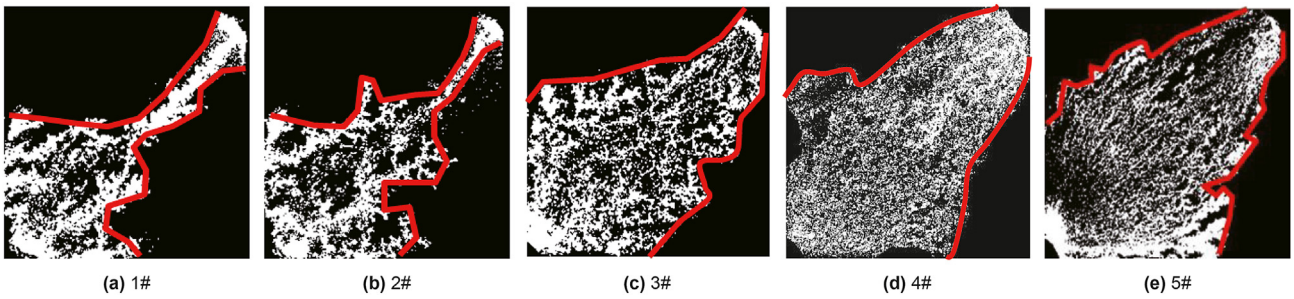

Fig. 13. Swept area of different processes.

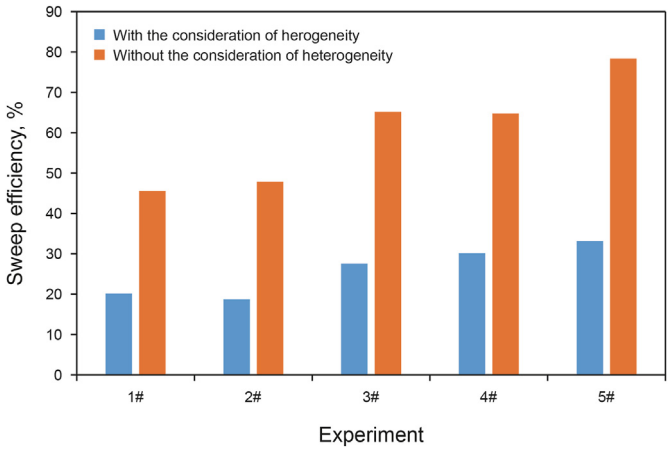

Fig. 14. Effect of microscopic reservoir heterogeneity on the sweep efficiency.

Fig. 19 shows the simulation results of temperature distribution at different times. As shown, compared with the experimental results in Fig. 16, a good agreement can be also observed. An obvious steam overlap is found. Simultaneously, after the injection of N_2/foam slug, during the 2nd steam flooding process, the angle of steam injection front is significantly increased, and the recovery performance is improved. Therefore, after a careful history match, this laboratory-scaled simulation model can be used to represent the actual 3D experiment, and it can be used to analyze the changing behavior of sweep range at different conditions.

(2) Vertical sweep efficiencies of different hybrid EOR processes

Based on the above laboratory-scaled numerical simulation model, the evaluation and analysis on the vertical and overall sweep efficiencies of different hybrid steam–chemical processes can be performed. During this process, the oil saturation is applied as an indicator to identify the sweep range, as shown in Fig. 20. For the reservoir region (grid) whose oil saturation is lower than 0.3, it can be identified as a swept area; the region whose oil saturation is between 0.3 and 0.6 is the influence area; the region whose oil saturation is higher than 0.6 is considered as the non-swept area. Therefore, based on the simulation results of oil saturation distribution, the sweep efficiencies at different conditions can be obtained. As shown, when the steam injection process lasts for about 436 min, a steam breakthrough phenomenon between injector and producer is observed. Thus, by calculating the ratio of swept area and entire reservoir, it is found that once a steam breakthrough is observed, the areal sweep efficiency is about 50.57% (top layer) and the vertical sweep efficiency is about 30.56% (interwell profile). It is in good agreement with the areal sweep efficiency obtained from the microscale visualized experiments (45.6%) (see Fig. 14). The minor difference between them is possibly caused by the limitation of critical oil saturation defined in this section. Simultaneously, from Fig. 20, it can be observed that the injection of N_2/foam slug can obviously increase the angle of oil saturation front and improve the vertical sweep efficiency. At the end of experiment, both the areal and vertical sweep efficiencies are improved.

Similarly, using this laboratory-scaled numerical simulation model, the vertical and areal sweep efficiencies of other steam–chemical processes in Table 2 can be also obtained, as

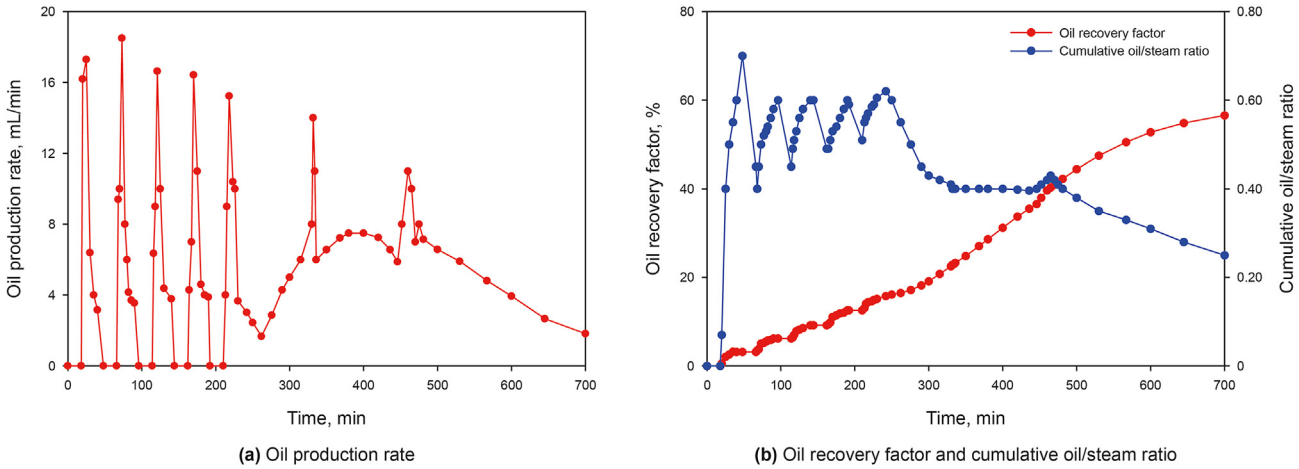

Fig. 15. Results of liquid production.

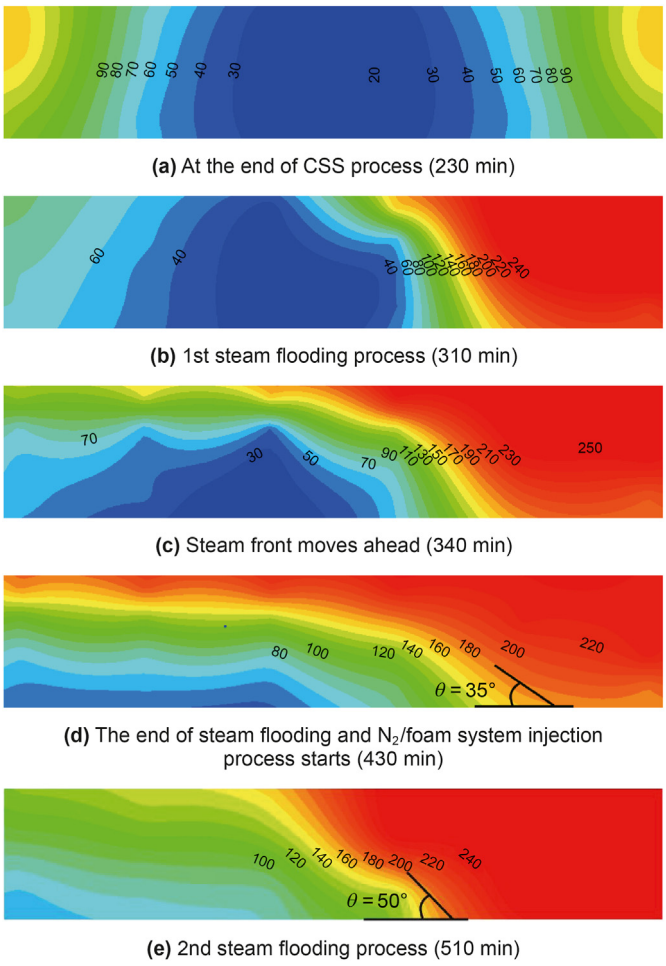

Fig. 16. Results of temperature distribution.

shown in Fig. 21. First, for hybrid steam–N_2 process (case 2#), compared with the pure steam injection process, the areal sweep efficiency of hybrid steam–N_2 process is slightly increased. and the vertical sweep efficiency is almost same as the pure steam injection. It is consistent with the results of microscale visualized experiments. Second, for hybrid steam–N_2/foam process (case 3#), as shown, its areal sweep efficiency is the lowest among the five processes. Its vertical sweep efficiency is improved by about 26% than the pure steam injection process. This is because that the injection of N_2/foam slug can significantly improve the shape of steam injection front and reduce the effect of steam overlap. Then, for hybrid steam–surfactant process (case 4#), its areal sweep efficiency (90.2%) is the highest among the five processes, and its vertical sweep efficiency is increased by about 6.5% than the pure steam injection process. The large difference between hybrid steam–surfactant process and hybrid steam–N_2/foam process is mainly caused by their different EOR mechanisms. For a hybrid steam–surfactant process, it can increase the microscopic displacement efficiency by reducing the interfacial energy between oil and water. On the other hand, it can also contribute to a slight increase in the sweep efficiency by *in-situ* emulsification. Therefore, from the results in Fig. 21, it can be observed that the sweep efficiency of case 4# is just slightly improved than the pure steam injection process. Last, considering both the advantages of N_2/foam system and surfactant solution, the hybrid steam–N_2/foam/surfactant process (case 5#) is proposed. From the results in Fig. 21, it can be observed that its areal sweep efficiency has reached about 86.3%, and the areal sweep efficiency is about 80.3%. The injection of N_2/foam slug can effectively improve the vertical steam injection profile and increase the vertical sweep efficiency. Then, the co-injection process of steam and surfactant can also improve the areal sweep efficiency. Therefore, case 5# has a good recovery performance in both areal and vertical directions.

3.4. Discussion on the EOR mechanisms of hybrid steam–chemical processes

Hybrid steam–chemical process is a typical EOR process for heavy oil reservoirs. It has been widely applied in the EOR processes of post steamed heavy oil reservoirs and the marginal heavy oil reservoirs. Based on the above experimental results, it can be found that a hybrid steam–chemical process can significantly improve the sweep efficiency both in vertical and areal directions. In this section, their EOR mechanisms can be summarized.

First, for a hybrid steam–surfactant process, based on the applied type of surfactant, its mechanisms are different. The surfactant used in this study is an oil soluble surfactant, also called as viscosity reducer. Therefore, in a heavy oil reservoir, its performance can be considered as a solvent. As shown in Fig. 22(b), a surfactant can interact with the oil film in a chief zone and reduce the interfacial energy. Simultaneously, from the color of oil film, it can be observed that the oil viscosity is reduced. Thus, the oil droplets/films formed during the pure steam injection stage will be unlocked. On the other hand, from the results of microscale

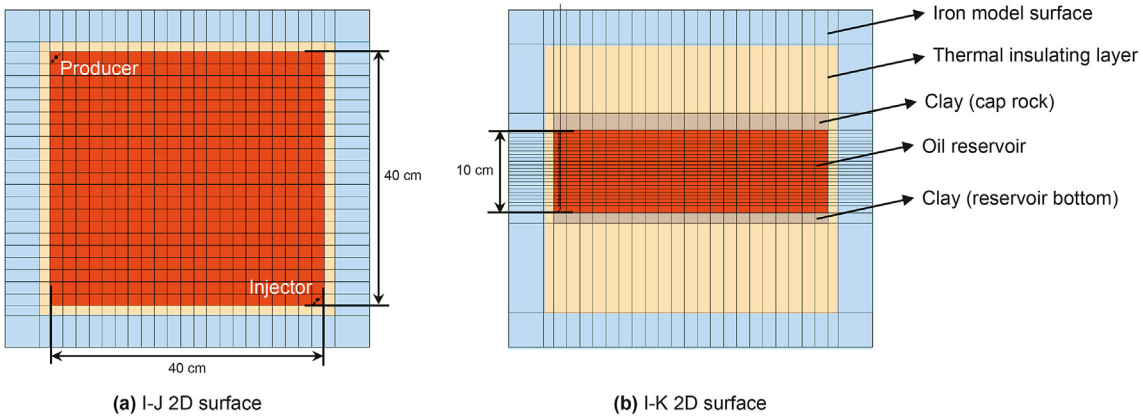

Fig. 17. The grid system of this laboratory-scaled numerical simulation model.

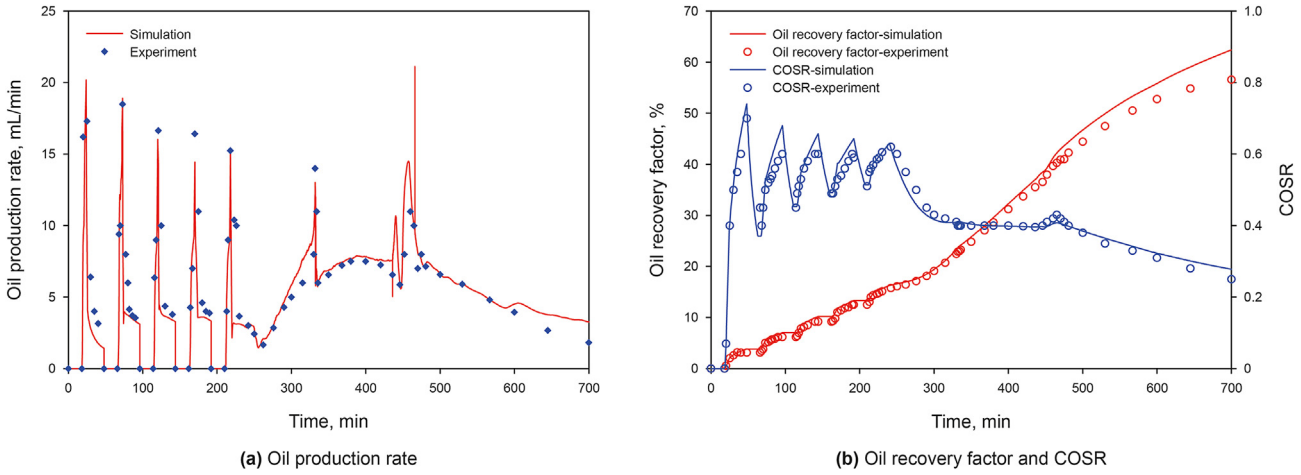

Fig. 18. The grid system of this laboratory-scaled numerical simulation model (COSR: cumulative oil/steam ratio).

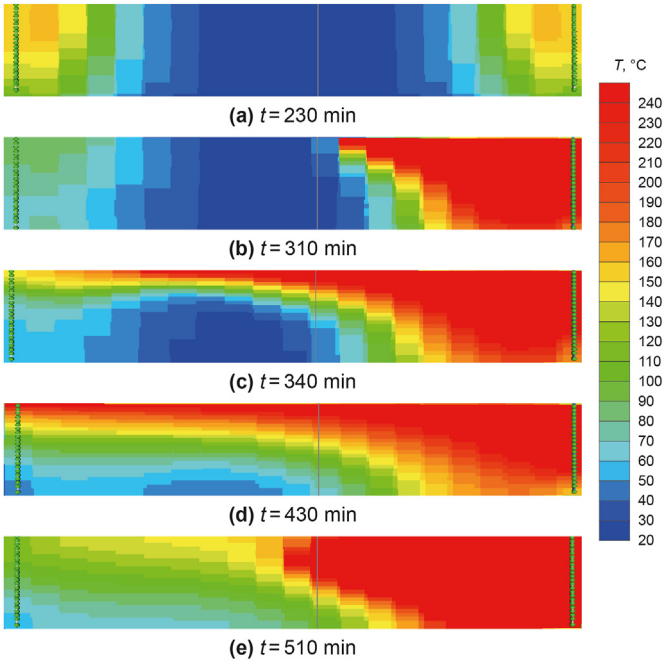

Fig. 19. Simulation results of temperature distribution.

visualized experiments, *in-situ* emulsification can be another important mechanism. As shown in Fig. 22(c), the oil/water emulsion in the micro-model can be accumulated both by a single droplet or by a cluster of droplets. Both of the two different forms can effectively plug the chief zone and increase the sweep efficiency.

Second, for a N_2/foam system, compared with hybrid steam–N_2 process, the addition of foaming agent can increase the membrane strength of gas bubble. As shown in Fig. 23(a), a cluster of N_2 foams can accumulate around the pore throat and plug the chief flow path of fluids. Therefore, from the results in Fig. 23(b) and (c), the previous chief fluid flow zone (A) will be plugged and the subsequent fluid injected will re-direct to another fluid flow path (B). This indicates that the sweep efficiency can be improved. Furthermore, from the results of macroscale 3D experiments (see Fig. 16), the effect of N_2/foam slug on the vertical sweep efficiency can be also observed.

4. Conclusions

In this paper, a systematic experimental investigation on the sweep efficiency of three hybrid steam–chemical processes is provided. From a microscale visualized model and a macroscale 3D model, both the vertical and areal sweep efficiencies are discussed. This study can provide an effective methodology to evaluate the sweep efficiency of different exploitation processes. On the other hand, based on the experimental observation, their EOR mechanisms of hybrid steam–chemical processes are also discussed. The main concluding remarks are provided as follows.

(1) From the static tests results, it is observed that although the foaming agent 2# has a lower maximum foaming volume and a lower half-life period, it can present a higher blocking capacity than foaming agent 1# at high temperature condition. For the surfactant (VR) used in this paper, it has a good thermal stability, and it can significantly reduce the oil viscosity at a low temperature condition (<100 °C).

(2) From the results of microscale visualized experiments, the areal sweep efficiencies of pure steam injection process and different hybrid processes are discussed. Among the tested four different hybrid processes, the process of a N_2/foam slug injection first and then steam–surfactant co-injection has the highest sweep efficiency. Simultaneously, from the collected 2D images, it is found that the microscale reservoir heterogeneity has an important effect on the calculation of sweep efficiency. Without the consideration of microscale reservoir heterogeneity, the areal sweep efficiency can be doubled.

(3) The macroscale 3D experimental results indicate that N_2/foam slug can effectively plug the steam breakthrough path between steam injection well and producer and improve the recovery performance. From the results of reservoir temperature distribution, it is found that the injection of N_2/foam slug can increase the steam front angle by about 15°, and the maximum oil production rate can be increased by about 50%.

(4) A laboratory-scaled numerical simulation model with the same data setting is developed. Based on this simulation model, a new method based on the oil saturation distribution is proposed to identify the sweep range. It is found that the areal sweep efficiencies obtained from the laboratory-scaled numerical simulation model are in good agreement with the results of microscale visualized experiment. A hybrid

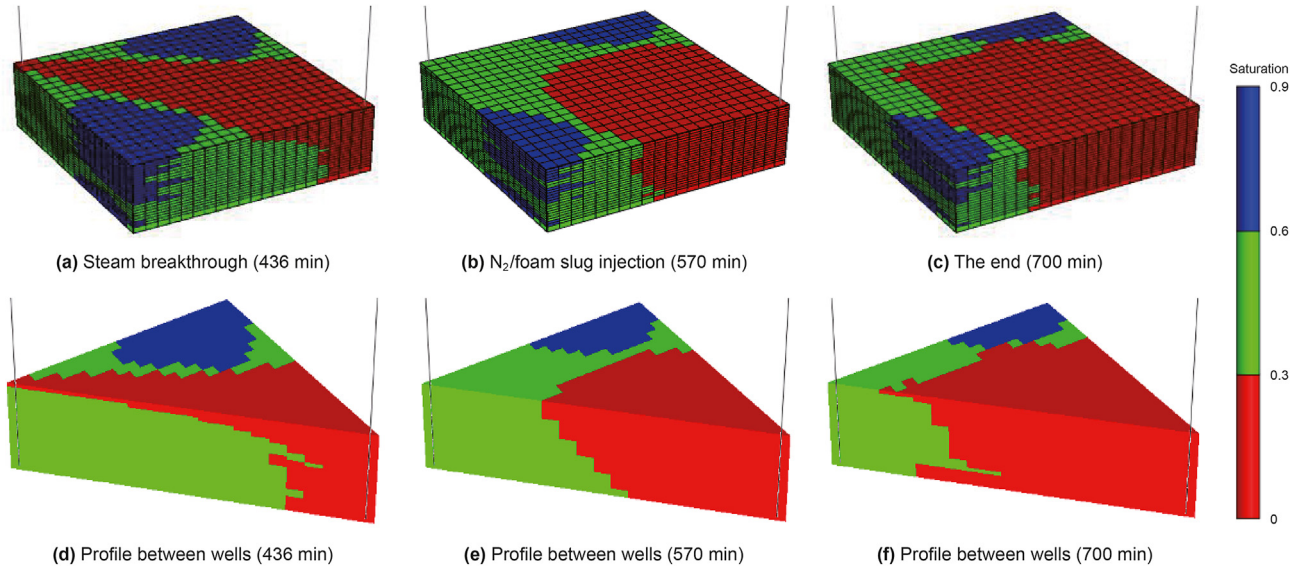

Fig. 20. Oil saturation distribution at different times.

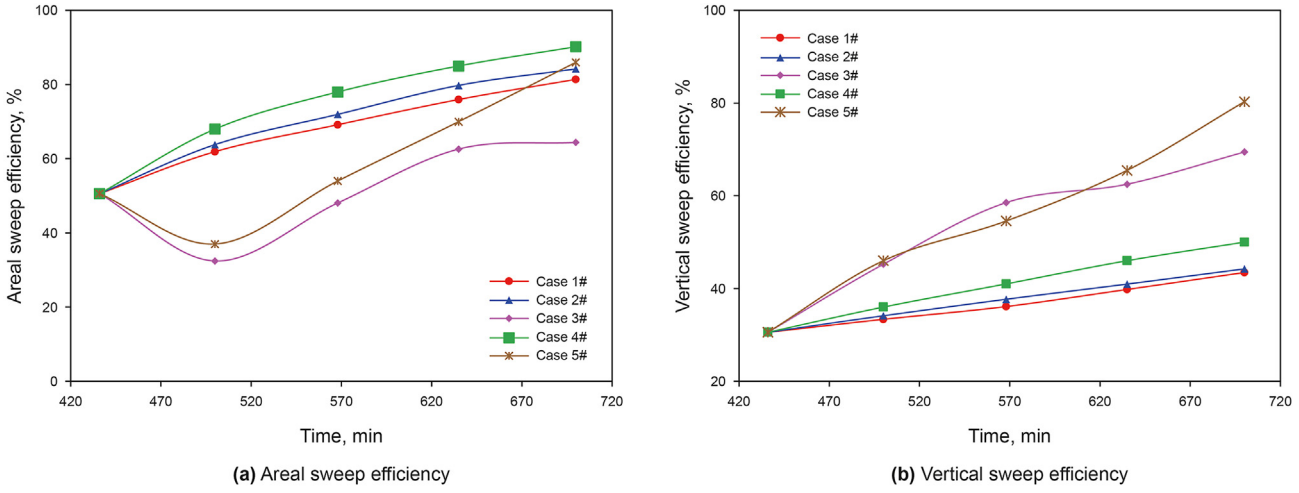

Fig. 21. Areal and vertical sweep efficiencies of different hybrid processes.

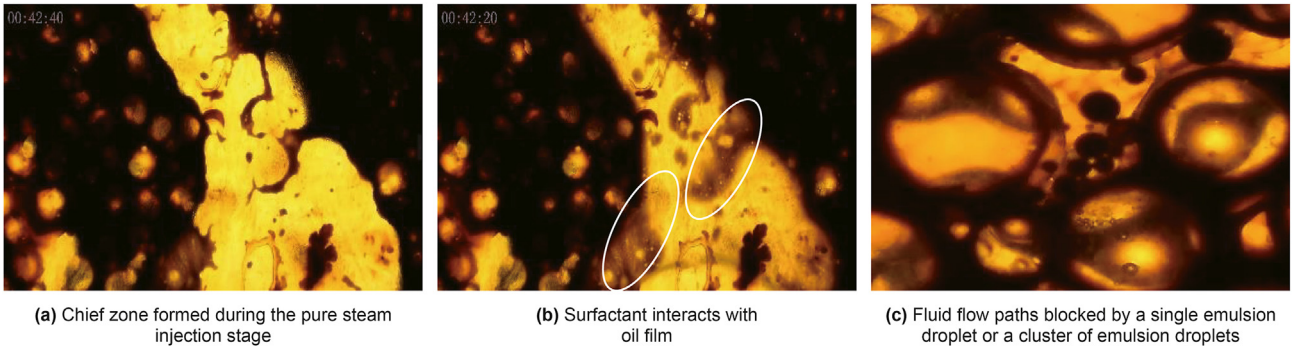

Fig. 22. Mechanisms of hybrid steam–surfactant process.

steam–N_2/foam/surfactant process has the highest sweep efficiencies in both vertical and areal directions. It indicates that a multiple hybrid EOR process is highly recommended than the single hybrid EOR process. Furthermore, combining the microscale and macroscale experimental results, the mechanisms of hybrid steam–chemical processes are also discussed.

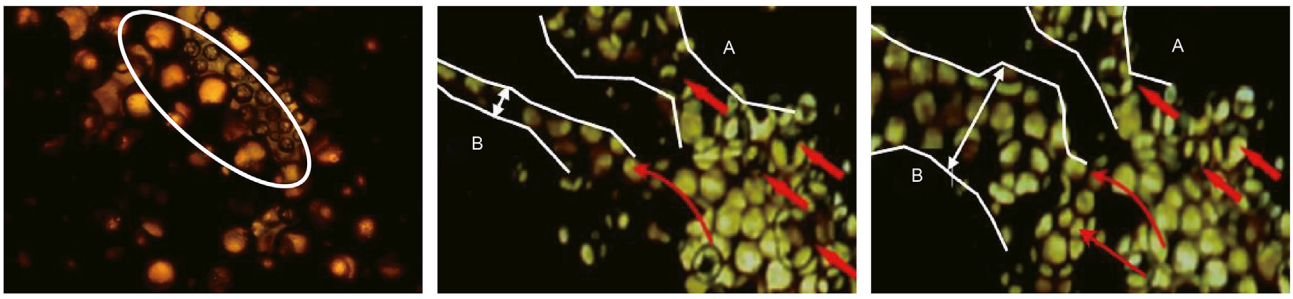

(a) A cluster of foam accumulated around the pore throat

(b) N_2/foam system flows along the path "A"

(c) Subsequent steam flows along another path "B"

Fig. 23. Mechanisms of N_2/foam system injection process.

Acknowledgements

This work was financially supported by the National Natural Science Foundation of China (U20B6003, 52004303) and Beijing Natural Science Foundation (3212020).

References

Adetunji, L.A., Ben-Zvi, A., Filstein, A., 2019. Foam formulation for high temperature SAGD applications. In: SPE Thermal Well Integrity and Design Symposium. https://doi.org/10.2118/198919-MS.

Ahmadi, M., Chen, Z., 2020. Challenges and future of chemical assisted heavy oil recovery processes. Adv. Colloid Interface Sci. 275, 102081. https://doi.org/10.1016/j.cis.2019.102081.

Alvarez, J.M., Han, S., 2013. Current overview of cyclic steam injection process. J. Petrol. Sci. Res. 2 (3), 116–127.

Ardali, M., Barrufet, M., Mamora, D.D., Qiu, F., 2012. A critical review of hybrid steam/solvent processes for the recovery of heavy oil and bitumen. In: SPE Annual Technical Conference and Exhibition. https://doi.org/10.2118/208966-MS.

Bashir, A., Haddad, A.S., Rafati, R., 2021. A review of fluid displacement mechanisms in surfactant-based chemical enhanced oil recovery processes: analyses of key influencing factors. Petrol. Sci. https://doi.org/10.1016/j.petsci.2021.11.021.

Bi, C., Wang, B., Bai, C., Tian, Y., He, Z., 2014. Application of nitrogen foam assisted steam flooding for the heavy oil reservoirs in Henan oilfield. Petrol. Geol. Eng. 28 (6), 115–117. https://doi.org/10.3969/j.issn.1673-8217.2014.06.036 (in Chinese).

Delamaide, E., Batôt, G., Ayache, S.V., 2020. Practical aspects of foam-assisted SAGD. In: SPE Latin American and Caribbean Petroleum Engineering Conference. https://doi.org/10.2118/199081-MS.

Delamaide, E., Cuenca, A., Chabert, M., 2016. State of the art review of the steam foam process. In: SPE Latin America and Caribbean Heavy and Extra Heavy Oil Conference. https://doi.org/10.2118/181160-MS.

Dong, X., Liu, H., Chen, Z., 2021. Hybrid enhanced oil recovery processes for heavy oil reservoirs. In: Developments in Petroleum Science. Elsevier.

Dong, X., Liu, H., Chen, Z., Wu, K., Lu, N., Zhang, Q., 2019. Enhanced oil recovery techniques for heavy oil and oilsands reservoirs after steam injection. Appl. Energy 239, 1190–1211. https://doi.org/10.1016/j.apenergy.2019.01.244.

Dong, X., Liu, H., Zhang, Z., Lu, C., Fang, X., Zhang, G., 2014. Feasibility of the steam-assisted-gravity-drainage process in offshore heavy oil reservoirs with bottom water. In: Offshore Technology Conference Asia. https://doi.org/10.4043/24763-MS.

Dong, X., Liu, H., Zhang, Z., Wang, L., Chen, Z., 2017. Performance of multiple thermal fluids assisted gravity drainage process in post SAGD reservoirs. J. Petrol. Sci. Eng. 154, 528–536. https://doi.org/10.1016/j.petrol.2016.12.032.

Dong, X., Wang, J., Liu, H., Zhang, Q., 2022. Experimental investigation on the recovery performance and steam chamber expansion of multi-lateral well SAGD process. J. Petrol. Sci. Eng. 214, 110597. https://doi.org/10.1016/j.petrol.2022.110597.

Fortenberry, R., 2013. Experimental Demonstration and Improvement of Chemical EOR Techniques in Heavy Oils. Master Thesis. University of Texas at Austin. http://hdl.handle.net/2152/26521.

Han, M., Xiang, W., Zhang, J., Jiang, W., Sun, F., 2006. Application of EOR technology by means of polymer flooding in Bohai Oilfields. In: International Oil & Gas Conference and Exhibition. https://doi.org/10.2118/104432-MS.

Huo, G.R., Li, X.M., Zhang, G.Q., 1999. Thermal Oil Recovery Technologies of Heavy Oil Reservoirs in Shengli Oilfield. Petroleum Industry Press, Beijing.

Jia, X., Dong, X., Xu, J., Chen, Z., 2018. Multiphase Fluid Flow and Reaction in Heterogeneous Porous Media for Enhanced Heavy Oil Production. John Wiley & Sons Ltd, pp. 319–351. https://doi.org/10.1002/9781119060031.ch6.

Keijzer, P.P.M., Muijs, H.M., Janssenvan, R.R., Teeuw, D., Pino, H., Avila, J., Rondon, L., 1986. Application of steam foam in the Tia Juana Field, Venezuela: laboratory tests and field results. In: SPE Enhanced Oil Recovery Symposium. https://doi.org/10.2118/14905-MS.

Khajehpour, M., Etminan, S.R., Goldman, J., Wassmuth, F., 2016. Nanoparticles as foam stabilizer for steam-foam process. In: SPE EOR Conference at Oil and Gas West Asia. https://doi.org/10.2118/179826-MS.

Ko, K.M., Chon, B.H., Jang, S.B., Jang, H.Y., 2014. Surfactant flooding characteristics of dodecyl alkyl sulfate for enhanced oil recovery. J. Ind. Eng. Chem. 20, 228–233. https://doi.org/10.1016/j.jiec.2013.03.043.

Liu, H.Q., 2013. Principle and Design of Thermal Oil Recovery Processes. Petroleum Industry Press, Beijing (in Chinese).

Liu, J., Zhong, L., Hao, T., Liu, Y., Zhang, S., 2022. Pore-scale dynamic behavior and displacement mechanisms of surfactant flooding for heavy oil recovery. J. Mol. Liq. 349, 118207. https://doi.org/10.1016/j.molliq.2021.118207.

Liu, Y.M., Zhang, L., Ren, S.R., Ben, B., Wang, S.T., Xu, G.R., 2016. Injection of nitrogen foam for improved oil recovery in viscous oil reservoirs offshore Bohai Bay China. In: SPE Improved Oil Recovery Conference. https://doi.org/10.2118/179584-MS.

Lu, C., Liu, H., Lu, K., Liu, Y., Dong, X., 2013. The adaptability research of steam flooding assisted by nitrogen foam in Henan Oilfield. In: International Petroleum Technology Conference. https://doi.org/10.2523/iptc-16678-MS.

Maaref, S., Kantzas, A., 2022. Nanoparticle assisted foam stability under SAGD conditions. In: SPE Canadian Energy Technology Conference. https://doi.org/10.2118/208877-MS.

Mahmoudi, S., Jafari, A., Javadian, S., 2019. Temperature effect on performance of nanoparticle/surfactant flooding in enhanced heavy oil recovery. Petrol. Sci. 16 (6), 1387–1402. https://doi.org/10.1007/s12182-019-00364-6.

Mendez, Z., Alvarez, J.M., Escobar, E., Colonomos, P., Campos, E., 1992. Cyclic steam injection with additives: laboratory and field test results of steam/foam and steam/solvent processes. In: SPE Annual Technical Conference and Exhibition. https://doi.org/10.2118/24632-MS.

Okoye, C.U., Tiab, D., 1982. Enhanced recovery of oil by alkaline steam flooding. In: SPE Annual Technical Conference and Exhibition. https://doi.org/10.2118/11076-MS.

Pang, Z., Liu, H., Zhu, L., 2015. A laboratory study of enhancing heavy oil recovery with steam flooding by adding nitrogen foams. J. Petrol. Sci. Eng. 128, 184–193. https://doi.org/10.1016/j.petrol.2015.02.020.

Pratama, R.A., Babadagli, T., 2022. A review of the mechanics of heavy-oil recovery by steam injection with chemical additives. J. Petrol. Sci. Eng. 208, 109717. https://doi.org/10.1016/j.petrol.2021.109717.

Shi, D., Yang, J., Yan, X., Zhang, B., Gu, K., 2005. Application of enhancing recovery factor by injecting nitrogen-foam in Shengli oilfield. Nat. Gas Explor. Dev. 28 (2), 47–49. https://doi.org/10.1117/12.2082966, 62, (In Chinese).

Sun, Q., Li, Z., Li, S., Zhang, N., Jiang, L., Wang, J., 2014. Oil displacement performance of stabilized foam system by SiO_2 nanoparticles. J. China Univ. Petrol.(Ed. Nat. Sci.) 38 (4), 124–131. https://doi.org/10.3969/j.issn.1673-5005.2014.04.018 (In Chinese).

Sun, X.F., Song, Z.Y., Cai, L.F., Zhao, Y.Y., Li, P., 2020. Phase behavior of heavy oil–solvent mixture systems under reservoir conditions. Petrol. Sci. 17, 1683–1698. https://doi.org/10.1007/s12182-020-00461-x.

Taghavifar, M., 2014. Enhanced Heavy Oil Recovery by Hybrid Thermal-Chemical Processes. Ph.D Dissertation. The University of Texas at Austin. http://hdl.handle.net/2152/24796.

Tiab, D., Okoye, C.U., Osman, M.M., 1982. Caustic steam flooding. J. Petrol. Technol. 34 (8), 1817–1827. https://doi.org/10.2118/9945-PA.

Wang, C., Li, Z., Li, S., Li, B., Ye, J., 2015. Experimental study on water control and oil recovery in bottom water driving reservoirs using plugging agents. J. China Univ. Petrol.(Ed. Nat. Sci.) 39 (6), 118–123. https://doi.org/10.3969/j.issn.1673-5005.2015.06.016 (In Chinese).

Wang, J., Liu, H., Ning, Z., Zhang, H., 2012. Experimental research and quantitative characterization of nitrogen foam blocking characteristics. Energy Fuels 26 (8), 5152–5163. https://doi.org/10.1021/ef300939j.

Wang, Y., Liu, H., Chen, Z., Wu, Z., Pang, Z., Dong, X., Chen, F., 2018. A visualized investigation on the mechanisms of anti-water coning process using nitrogen

injection in horizontal wells. J. Petrol. Sci. Eng. 166, 636–649. https://doi.org/10.1016/j.petrol.2018.03.083.
Wang, Y., Liu, H., Guo, M., Shen, X., Han, B., Zhou, Y., 2021. Image recognition model based on deep learning for remaining oil recognition from visualization experiment. Fuel 291, 120216. https://doi.org/10.1016/j.fuel.2021.120216.
Wu, Z., Liu, H., Wang, X., Zhang, Z., 2018. Emulsification and improved oil recovery with viscosity reducer during steam injection process for heavy oil. J. Ind. Eng. Chem. 61, 348–355. https://doi.org/10.1016/j.jiec.2017.12.033.
Zhang, F.L., Zhao, H.Y., 2007. Steam Based Recovery Technologies of Heavy Oil Reservoirs in Liaohe Oilfield. Petroleum Industry Press, Beijing (in Chinese).